

BALANCES

Balances are usually considered devices that weigh. Here, we will take a more general approach because even the ordinary beam balance in school laboratories uses one force balanced against another, so that static equilibrium of the device is maintained. More generally, then, a balance is a device that determines an unknown force by balancing a known or calibrated force. For example, lever-arm balances use a known mass at a known position to measure an unknown mass at a known location. Spring balances use the displacement of a spring with known elastic properties to measure unknown forces. A modified version of a spring balance is the cantilever-type, where an elastic arm supported at one end bends under load. Another related class of balances is the torsion balance, in which a thin torsion fiber suspends a beam that twists because of forces solely in a horizontal plane. The amount of twist per unit torque is determined by the elastic properties of the fiber. The principles governing the various balance types are discussed more thoroughly in the following subsections.

Many commercial balances available today have automated recording systems, so that force signals are converted either to electrical voltage or current. Specialized precision balances for measuring masses of minute quantities, investigating chemical reactions, or studying gaseous-phase processes have also benefited from automation. Automation allows continuous monitoring of experimental variables as well as measuring in environments such as vacuums. Instrumentation typical of automated balances is discussed in the next section.

The last section describes recent designs for microbalances and vacuum microbalances. Before the 1960s, a vacuum microbalance typically consisted of a lightweight beam, counterbalanced by an electromagnetic force. As mass is added to one end of the beam, feedback on the beam deflection maintains equilibrium, usually electromagnetically. This feedback signal, proportional to the mass increment, is read as the mass measurement. Although similar microbalances are still in use, microbalances based on quartz-crystal oscillators are more common today, where mass increments translate into resonance frequency shifts. Recent designs of microbalances are described later.

Lever-Arm, or Beam Balances

By far, these are the most common balances in academic laboratories. Beam balance weigh an unknown mass through can-

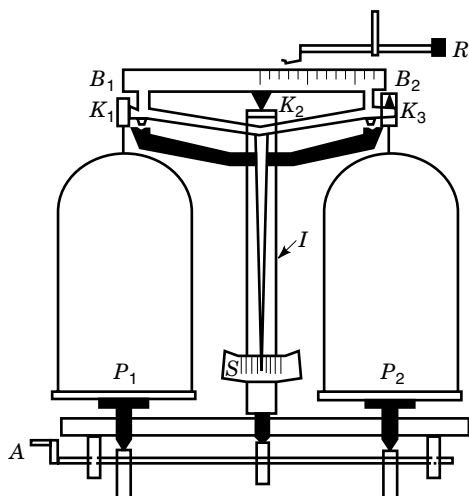


Figure 1. The beam balance. The unknown sample is placed in pan P_1 . Standard weights are added to pan P_2 to return the beam to the null position read from scale S . Masses smaller than 10 g are effectively added to beam B_2 through the rider R .

cellation of the gravitational torque caused by placing the mass a known distance from the fulcrum of an extended beam. Figure 1 depicts such a balance, in which the canceling torque is provided by a known mass placed a known distance away from the fulcrum.

Because this balance has components found even in more modern automatic beam balances, its operation is discussed further here. The unknown mass is to be placed in pan P_1 , and the balance weights, or standards, are then loaded into pan P_2 until the needle indicator I swings equally about the center of scale S . The center of gravity of the system falls above knife-edge K_2 in equilibrium. Knife-edges are used to lower friction that may cause the swinging motion to stick in a position other than true equilibrium.

Because masses less than 10 g are difficult to handle (and it is undesirable to handle them because any small deposits change the mass), small weights are usually incorporated in a rider system, denoted in Fig. 1 by R . A small mass of 10 g is loaded by the rider onto beam B_2 at any position closer to the fulcrum than the pan. In the balance shown, beams B_1 and B_2 are equal length, so that loading a 10 g mass at the end of B_2 gives a reading of 10 g. Thus, loading the 10 g mass at a position 0.1 of the distance out from knife-edge K_2 gives a reading of 1 g. Multiple-beam analytic balances use multiple rider systems, so that the standard weights are never handled physically.

Beam balances also use an arrestment device, labeled A in Fig. 1. This device allows attaching the weighing pans rigidly to the supporting structure, so that the pans are released slowly near equilibrium, after loading is accomplished. Releasing A sets the balance into swinging motion, so that the position of the indicator may be monitored.

Two other common features are not shown explicitly in this figure: taring and damping. Taring is necessary because inevitable differences in the masses of pans P_1 and P_2 would cause a nonzero reading even with the balance unloaded. Taring is often accomplished with a counterweight mounted on one of the beams by an adjustable screw, so that the taring torque

can be adjusted. Although a large amount of friction is undesirable in the knife-edge itself, damping the swinging motion of the scale indicator is desirable to reduce the time needed for a reliable measurement. Damping is often incorporated by placing small magnets near the end of one beam and using the eddy-current brake effect to damp the motion.

The sensitivity of the balance is fixed by the length of the indicator needle I , the unit measurement on the scale S , the size of the smallest mass placed in the rider system, and the increments on the rider scale. The balance is also more sensitive if the two beam arms are longer, but this increases the period of swinging caused by an increase in the moment of inertia of the balance. Practical beam balances, such as those manufactured by Mettler, measure from hundreds of grams to less than 0.0001 g.

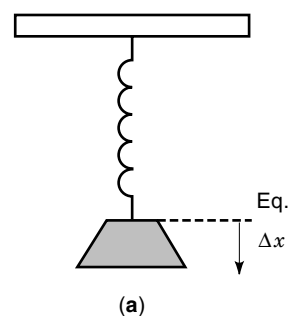
Cantilever and Spring Balances

Both cantilever and spring balances use the elastic forces produced by a known material to balance an unknown weight. In a spring scale [Fig. 2(a)], loading an unknown mass stretches the spring beyond its unstretched length a distance Δx . The weight of the mass is related linearly to this displacement by Hooke's law:

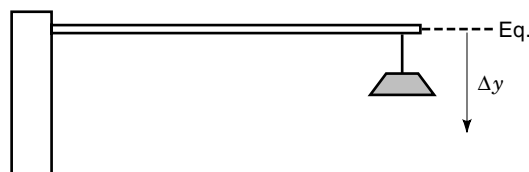
$$F = k\Delta x$$

where k is the elastic spring constant. This relationship arises from the strain on the spring material, which is [Fig. 3(a)] related to a compressive or stretching force F applied perpendicularly to one end of a wire of cross-sectional area A via

$$\frac{F}{A} = Y \frac{\Delta x}{L}$$



(a)



(b)

Figure 2. Spring (a) and cantilever (b) balances counter the weight with internal restoring forces. The displacement of the balance is proportional to the load over a wide range, where the constant of proportionality is called the effective spring constant k .

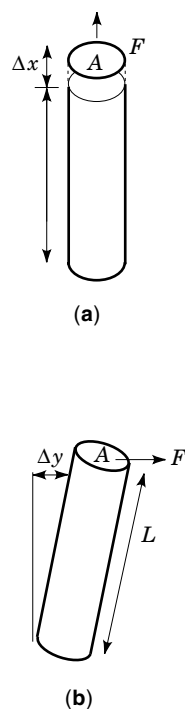


Figure 3. Two linear material deformations that may be exploited in balances. (a) Strain corresponds to an elongation in a fiber caused by a force applied perpendicularly to a cross section. (b) Stress corresponds to a sideways displacement of the fiber caused by a force applied parallel to a cross section.

where L is the length of the wire and Y is Young's modulus for the wire material. Spring balances are made of very stiff materials, such as steel, tungsten, or quartz, with elastic moduli close to 10^{11} N/m². The previous strain relationship indicates that one can make a more sensitive spring balance by increasing the length L of the spring; and by reducing the cross-sectional area A , one can make the deflection of the balance larger for a given applied force.

In a cantilever balance, mass is loaded onto the end of a flexible rod or bar, mounted horizontally [Fig. 2(b)]. As in a spring scale, the deflection of the end of the rod is proportional to the weight added. This can be deduced by considering the shear force F acting on the fiber end [Fig. 3(b)] in the plane of the rod's cross-sectional area A :

$$\frac{F}{A} = G \frac{\Delta y}{L}$$

where Δy is the vertical deflection of the rod and G is the shear modulus of the material (typically the same order of magnitude as Y). As in spring balances, cantilever balances are made more sensitive by increasing the length of the rod and reducing the cross-sectional area.

Spring and cantilever balances are calibrated by loading standard masses onto the balance, while measuring the corresponding set of displacements. The data set allows determining k , the effective elastic constant of proportionality. When unknown masses are to be determined, they must be within the range of masses used for calibration, because both springs and cantilever beams are linear over only a limited range of loads.

Another method for calibrating spring and cantilever balances requires that they serve as high-Q (i.e., low-friction) mechanical oscillators. For a highly underdamped spring system, the resonant frequency of oscillation is given in Hertz by

$$f = \frac{1}{2\pi} \sqrt{\frac{k}{m}}$$

If frequency difference measurements of 1 ppm are reliably and repeatedly made on an oscillating mass, a mass change of 2 ppm can be detected.

Torsion Balances

Two types of balance are denoted by this title. In one type, similar to a beam balance, a taut wire is used as a fulcrum in place of a knife-edge [Fig. 4(a)]. Like other analytical balances, this balance measures a gravitational torque by a downward angular deflection $\Delta\theta$ of the beam.

A more commonly used torsion balance relies on the elastic properties of a fiber to determine small forces acting to rotate a beam. A beam of arm R is supported from its center of gravity by a wire or fiber w [Fig. 4(b)]. Forces apply a couple simultaneously to both ends of the beam, which rotates through an angle $\Delta\psi$. The total torque Γ and $\Delta\psi$ are related through $\Gamma = \kappa\Delta\psi$, where κ is an elastic constant determined by the shear modulus of the fiber G , the length of the fiber l , and the fiber radius r :

$$\kappa = \frac{r^4}{l} G$$

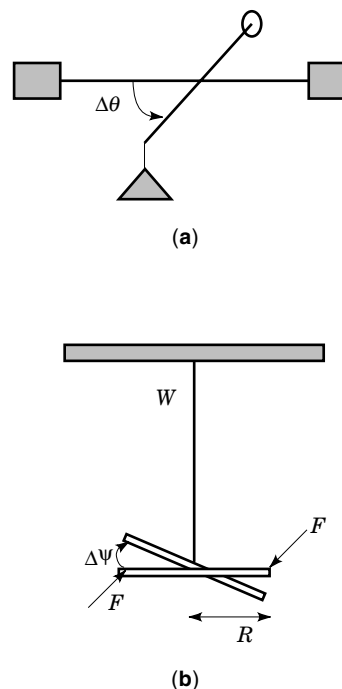


Figure 4. Two types of balances called torsion balances. (a) This is most similar to a beam balance because a weight added to one end creates a downward deflection of a beam. The torsion wire takes the place of a knife-edge. (b) This torsion balance is most similar to spring and cantilever balances. Material properties of the wire w balance the torque tending to twist the beam in a horizontal plane.

Thus, one can see that this form of torsion balance is most similar to spring and cantilever systems, in that known material properties of the fiber produce the balancing forces. Also, like these other balances, a torsion balance can be made more sensitive by increasing the fiber length and reducing the wire radius.

Torsion balances are unique in that they are designed to measure forces occurring in a horizontal plane. They are calibrated by using the frequency of oscillation of the beam about its unperturbed equilibrium position. (Practical torsion balances have periods that are several seconds to several minutes long.) The natural torsion frequency is given by

$$f = \frac{1}{2\pi} \sqrt{\frac{\kappa}{I}}$$

where I is the moment of inertia for the beam twisting in a horizontal plane about the fiber point of suspension. This I must be calculated or measured independently to determine κ .

Applications of the torsion balance have been numerous and include determining the Newtonian gravitation of constant G and the magnetic properties of superconductors. Such applications require sensitivities of 10^{-9} N·m/rad, which are readily achieved in many laboratories.

INSTRUMENTATION

There are two main types of balance in terms of how measurements are acquired: null-detection and deflection type. In deflection-type balances, force or mass measurements are related to how far the balance moves from an equilibrium position. Cantilever and spring balances fall in this category. If such balances are to be automated, a position transducer is needed to convert a deflection into an electrical signal. In

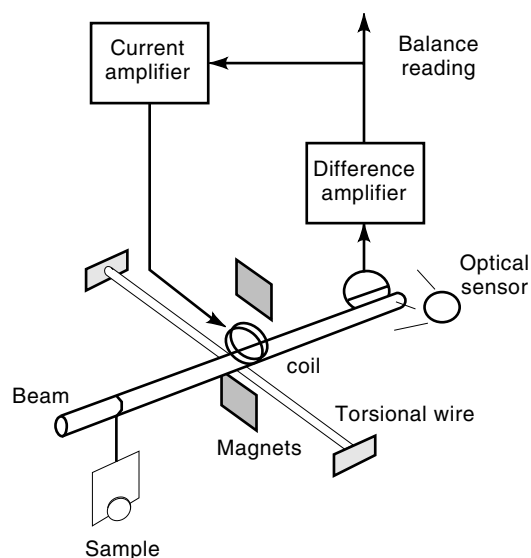


Figure 5. A null-detection microbalance. Position sensing is accomplished optically, and feedback is provided through the energized coil on the beam that attempts to align with the field created by the stationary magnets. Such balances are capable of detecting mass increments as small as 10^{-7} g.

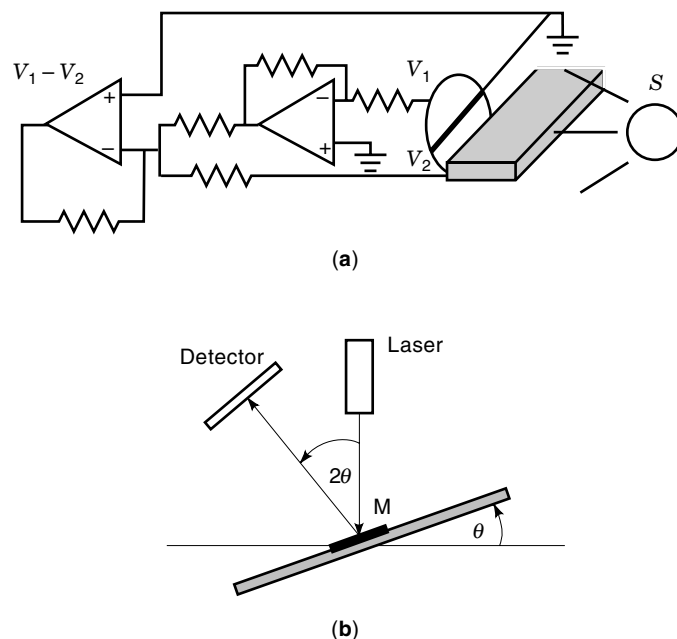


Figure 6. Optical position sensing. (a) Split photodiode. If all resistors shown have equal value, the output of the second operational amplifier is proportional to the difference in the detector outputs. (b) Reflection, or optical lever-arm device.

null-detection balances, the balance is to be maintained in equilibrium, and the force needed to restore the balance is read as the measurement. Beam balances are of this variety. Automated null-detection balances require a negative feedback loop. A position transducer converts a displacement into an electrical signal, which is fed back to a force-producing mechanism that restores equilibrium. Figure 5 shows a Cahn beam microbalance, in which an electromagnetic coil energized by an optical position sensor tries to maintain alignment with the field created by static magnets. Because position sensing is central to both deflection and null-detection balances, various transducers are described below.

Optical Detection

One common method for sensing the position of a beam balance uses a light source and split photodiode arrangement [Fig. 6(a)]. The photodiode outputs a voltage signal proportional to the difference in source light intensity S reaching its two separate halves. The beam balance is set so that, at equilibrium, it covers both halves of the split photodiode symmetrically. As the beam moves upward, the lower half of the detector is more illuminated than the upper half, and the photodiode output changes accordingly. Many balance position-detecting systems use a similar split-transducer arrangement. Relatively simple, inexpensive circuits can be developed, such as the one shown, that output a voltage proportional to the difference between the two detector halves. Hence, the transducer output is null at equilibrium and produces a bipolar signal dependent on the direction of displacement.

Reflection is often used with balances that create angular deflections, such as cantilevers, beam balances, and torsion balances. In such systems, a well-collimated intense light

source, such as a laser, is reflected from a mirror attached to the pivoting body or movement arm [Fig. 6(b)]. As the balance arm moves through an angle θ , the beam is deflected through 2θ . As the balance pivots, the light beam traverses an arc, the length of which is determined by how far the detector is placed from the balance. The length of this optical lever arm determines the sensitivity of the position transducer.

Two types of sensors are available for measuring the deflected light beam: linear charge-coupled device (CCD) arrays and position-sensing devices (PSDs). A CCD array consists of a set of photosensitive elements, typically a few microns in size. Arrays are commercially available with thousands of so-called pixels. The device produces a digital signal that provides information about the light intensity recorded as a function of discrete position along the one-dimensional array. This method is limited in resolution by the number of photosensitive elements in the array and also requires some computer processing to determine the centroid of the laser light spot. Thus, resolution in such devices is gained at the expense of speed. The second type of detector, the PSD, consists of a single photodiode several cm in length. A resistor network built into the device behaves as a voltage divider, so that the device output is related to the position of the laser spot on the photodiode active area. Unlike the CCD array, the signal is continuous, and no centroid determination is required. However, a specialized analog circuit is required to make the voltage output proportional to the beam-spot position on the device. PSDs are available that measure $0.1 \mu\text{m}$ of linear motion.

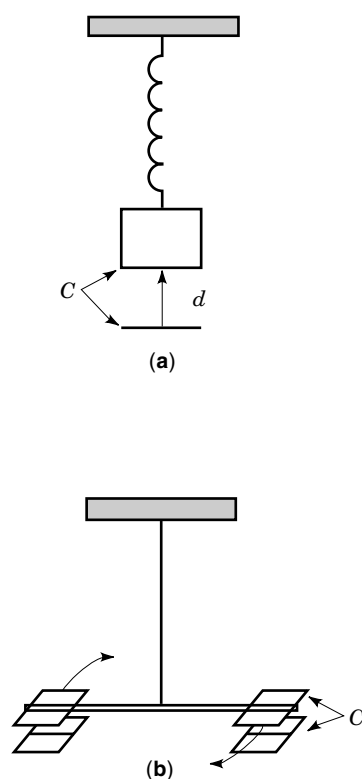


Figure 7. Two types of capacitive position sensors. (a) The capacitance decreases as the separation between the two plates increases with balance motion. (b) The area of overlap between the capacitor plate on the beam and the split capacitor sensors changes as the balance rotates.

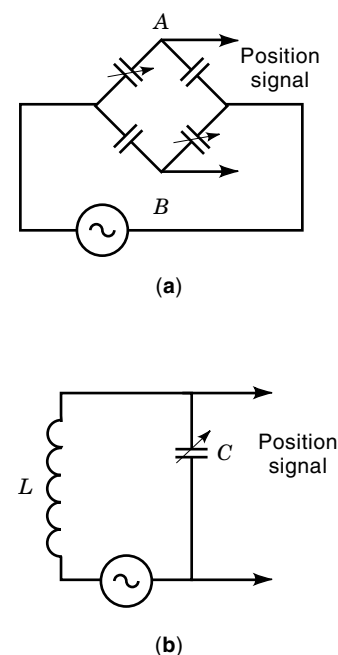


Figure 8. Two circuits used to change capacitance variations into an electrical signal. (a) Ac capacitance bridge, in which a moving capacitor plate deflects across a split capacitor plate (two variable C s). (b) Resonant LC circuit.

Capacitive Sensing

Capacitors store electric charge and energy. A capacitor consists of two conductors separated by an air gap or dielectric. How much charge the two conductors store is determined by the shape and size of the conductors and by the geometry of the gap separating them. These features can be used to convert motion into an electrical signal.

The simplest configuration is the parallel-plate capacitor, the capacitance of which is determined by the area of the plates A and gap size d :

$$C = \frac{\epsilon_0 A}{d}$$

where ϵ_0 is the permittivity of free space (8.85×10^{-12} F/m). The small value of ϵ_0 means that position transducers using capacitors must be very sensitive to minute changes in C of the order of nanofarads or picofarads.

Two types of capacitive position sensors can be developed, depending on whether the gap changes [Fig. 7(a)] or the area of the plates changes [Fig. 7(b)] as the balance moves. [Figure 7(b)] indicates that although the movable capacitor plate is single, the stationary plate consists of a split conductor. For the same reason that split photodiodes are used in optical sensors, split capacitor plates allow determining the direction of balance movement.

One also needs a circuit designed to detect changes in C . This is often done by placing the variable position-sensing capacitor in an ac-excited bridge [Fig. 8(a)]. The potential difference between points A and B in the figure remains null, as long as the four capacitors in the bridge have equal values. As the variable C s change because of motion of the balance, the amplitude and phase of the voltage difference ($V_A - V_B$)

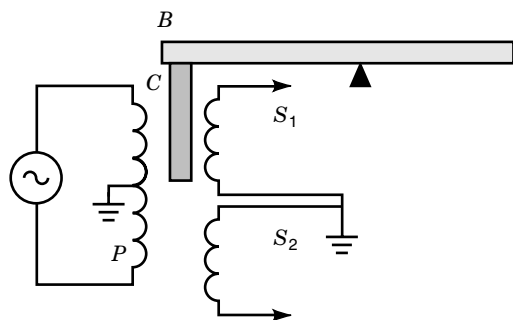


Figure 9. Linear variable differential transformer (LVDT), an inductive position sensor. The center-tapped primary coil P is flux-coupled to the secondary windings through an iron core C . As the beam B deflects up or down, either S_1 or S_2 becomes more strongly coupled to the primary.

changes correspondingly. Another common arrangement is to place the capacitive position sensor in a resonant LC circuit [Fig. 8(b)], excited by an ac source driving the circuit near the resonant frequency of the circuit, given by $1/(2\pi\sqrt{LC})$. As the capacitance changes, the amplitude and phase of the voltage drop across C also change.

Strain Gauges

Strain gauges are devices that convert physical elongation or compression into an electrical signal. They are readily incorporated into deflection-type balances, such as the spring scale and beam balance. A strain gauge consists of four metal-film resistors placed in a Wheatstone bridge configuration. As the balance deflects, the resistors deform and destroy the bridge electrical balance. It is difficult to find strain gauges that measure small displacements reliably, so that these devices are more appropriately used in balances designed to measure large loads, hundreds of grams to thousands of kilograms.

Inductive Sensing

A common technique for measuring deflection in balances is a device known as a linear variable differential transformer (LVDT). As all transformers contain a pair of coils coupled with an iron core, so do LVDTs. However, the primary coil, the one to be excited directly with an ac source, is center-tapped. This allows two secondary coils to share a common ground at the center of the transducer (Fig. 9). This configuration is reminiscent of the split photodiode sensor described previously, so it is evident the LVDT is capable of determining the direction of balance motion. The iron core is attached to the balance beam and is centered at equilibrium. As the beam displaces upward, coil S_1 in the secondary is more strongly coupled to the primary than coil S_2 . The voltage signals from the two secondary windings are processed by an electronic circuit that produces a signal proportional to their difference.

MICROBALANCES AND VACUUM MICROBALANCES

A microbalance is a device that either determines a small mass (μg range) or force. Applications are numerous, including measurement of adsorbed chemicals on surfaces, film

thicknesses in vacuum deposition systems, minute pressure changes, dehydration and hygroscopic processes, pyrolytic reactions, corrosion, etc. Measurement in vacuo is often necessary, to remove buoyancy or chemical reactions that cannot be controlled. Under these conditions the balance is termed a vacuum microbalance. The main difference between a vacuum microbalance and other such devices is that the balance parts must be capable of being heated to high temperature to circumvent outgassing and appropriate mechanisms for loading and reading must be placed within the vacuum chamber.

As was mentioned in the previous section, most microbalances before 1960 were similar in design to standard automated balances. Differences were required in the small, delicate parts, from which beams, springs, and cantilevers were machined, and the low levels of signals produced by the position transducers. In this section, relatively new forms of the microbalance are presented. Two of these, the quartz crystal microbalance (QCM, described later) and the surface acoustic wave (SAW, described later) microbalance, are based on the piezoelectric nature of quartz. When a quartz crystal is placed in a sufficiently strong electric field, it undergoes a characteristic deformation. Oscillating quartz crystals can be made sensitive to small material deposits on their surfaces.

Atomic-force microscopy is also an unfolding field, in which a miniature cantilever beam records forces on a microscopic scale. If such a device is used to create images of materials, it is a microscope. However, if such a device is used to measure forces absolutely, it is a microbalance.

Atomic Force Balances

An atomic force microscope (AFM) has at its heart a micro-machined cantilever beam, which responds to microscopic forces as it is dragged over a surface or through a fluid. Although cantilever fibers and leaves have also been used to measure small forces, currently V-shaped structures of Si_3N_4 are popular because they resist lateral motion and the tendency to twist. These beams are only tens of micrometers thick and hundreds of micrometers long.

Regardless of the shape of the cantilever beam, a remaining challenge for such small devices is calibrating them to determine their effective spring constants. One technique involves calculating the k from the size of the cantilever and its bulk properties (namely, the Young's modulus of the material from which it is made). However, this calculation is unreliable because the thin films may not have the same Young's modulus as large blocks of material. Another problem concerns the fact that many cantilever beams have gold surfaces sputtered on them to make them easier to track via optical reflection. The gold film also changes the Young's modulus in a way that is difficult to determine.

Another method of calibrating these cantilever beams involves loading the end of the beam with mass and measuring the beam displacement or the shift in the resonant frequency of the beam set into oscillation. Both methods are common to calibrating any spring-type balance. However, for atomic force balances this is a destructive method, as glue is often necessary to attach a μg mass to the beam. It has also been found that the effective spring constant measured by mass loading and frequency shifting is affected by the attachment location. New methods of calibrating these cantilevers to determine

microscopic forces will continue to develop, as AFMs become more widely used for absolute force measurements.

Quartz Crystal Microbalances

Quartz crystal microbalances (QCMs) are extensively used in materials research and in chemistry laboratories. Their longest application has been for film-thickness monitoring during vacuum deposition. More recently, they have been adapted for investigating liquid solutions, in which chemical reactions at the liquid-quartz interface leave deposits only one atomic layer thick.

QCMs are an attempt to use frequency measurement as a mass indicator. A thin (several hundred micrometer) wafer is cut from a quartz crystal, and typically gold electrodes are deposited on both faces of the wafer [Fig. 10(a)]. Shear-mode oscillations are set up in the wafer when an oscillating electric field is applied to the electrodes [Fig. 10(b)]. If the thickness of the wafer is one-half the wavelength of the shear-mode fundamental, the antinodes of the oscillation occur at the faces of the wafer. In this case, very little energy loss occurs at the wafer faces, and the acoustic wave essentially becomes trapped inside the wafer. Constructed in such a way, a quartz crystal oscillator can have a very high Q , and thus a narrow resonance frequency of oscillation.

When quartz wafers are prepared, care is taken to minimize the dependence of this natural frequency of oscillation on temperature. Such a dependence causes errors in thickness monitors because mass deposition is usually measured as a change in the resonant frequency. QCMs are manufactured with an AT cut, a particular crystallographic orientation known to minimize temperature dependence of the resonant frequency at room temperature (see Fig. 11).

The resonant frequency of an AT-cut quartz crystal is given as $f = A/d$, where d is the thickness of the wafer and A is a constant, 1.67 MHz-mm. The initial thickness of the wa-

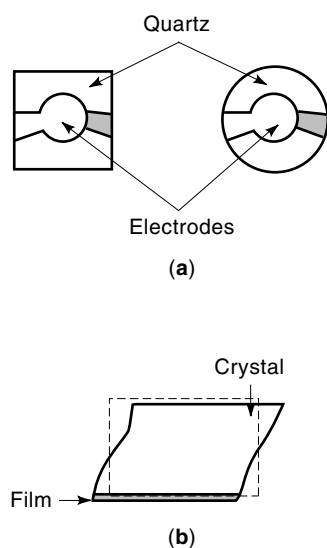


Figure 10. Operation of the quartz crystal microbalance. (a) Quartz wafers showing electrodes. The dark gray region indicates the orientation of the electrode on the opposite side of the wafer. (b) Shear oscillation in the bulk of the quartz crystal. As long as the film deposit is thin compared with the crystal width, the shear wave is damped very little by the film.

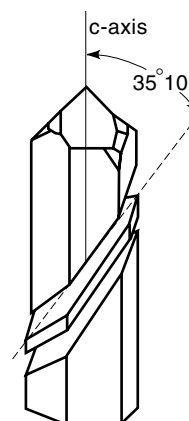


Figure 11. Orientation of an AT-cut wafer in a quartz crystal.

fer is cut to give f near 10 MHz. Smaller cuts produce a higher frequency but reduce both the sensitivity of the crystal and the thickness of foreign material that can be practically deposited.

Mass deposits Δm on the QCM are monitored according to the Sauerbrey relationship:

$$\Delta f = -2.3 \times 10^6 \frac{\text{cm}^2}{\text{Hz} - g} f_0^2 \frac{\Delta m}{A}$$

where A is the area over which the film has been deposited, and Δf is a measured shift in the quartz oscillation frequency. This relation shows explicitly that the QCM becomes more sensitive to deposits as the natural frequency f_0 of the crystal increases.

Several well-studied problems occur in using QCMs, both in vacuum deposition systems and in electrochemical environments. One difficulty arises from the sensitivity of the QCM to varying environmental conditions other than a change in thickness, especially to temperature changes and variations in liquid viscosity and density. The main difficulty in using QCMs as film-deposition monitors in vacuum is the fact that the evaporated substance conveys thermal energy to the crystal, thereby changing its temperature. Even if it is an AT-cut crystal, the crystal has a frequency dependent to a slight degree on temperature. The way around this problem is to place a shutter close to the crystal surface, so that the film does not cover the entire crystal surface. Also, the shutter is not opened immediately, so that the crystal has time to reach thermal equilibrium before thickness is monitored.

Another well-documented problem is that the crystal's sensitivity to thickness changes is not uniform across the wafer. The sensitivity is highest in the center and lowest on the periphery. The profile may be made more uniform by polishing the crystal so that it exhibits a convex or plano-convex shape. However, most researchers take care to confine reactions and deposits to the area of the wafer covered by the electrode.

One final challenge to using QCMs concerns the approximation that the nature of the shear wave is not affected by the film deposit but that only the speed of the wave changes. In reality, the film changes the acoustic impedance at the surface, which in turn affects energy loss of the wave.

As a foreign substance is deposited on one face of the crystal, the thickness of the wafer increases, and the resonant frequency drops. As long as the foreign film is thin compared with the wafer thickness, the elastic properties of the foreign substance do not affect the behavior of the shear wave. Thus only the areal mass density affects the frequency. This approximation has been experimentally verified, as long as the foreign film remains thinner than a few percent of the wafer thickness. It is advisable to clean the wafer after a certain amount of deposit has accumulated, although a technique called Z-match, described in the next paragraph, allows larger deposits.

A more careful one-dimensional acoustic analysis of the shear wave propagating through the crystal recognizes the impedance mismatch at the boundary between the film and the quartz. In this instance, a transcendental equation relates the frequency shift of the oscillator to the mass deposited Δm on the crystal:

$$\Delta m/m_0 = -\frac{z_f f_0}{z_Q \pi f} \arctan \left(\frac{z_Q}{z_f} \tan \frac{\pi f}{f_0} \right)$$

where z_f and z_Q represent the acoustic impedances of the film and quartz materials, respectively, and m_0 is the initial mass of the crystal. Third-generation thickness monitors use this relationship, which is valid up to loads of 70% of the quartz mass. A disadvantage to using this Z-match technique is that the ratio of the two impedances must be determined by an independent measurement and entered in the deposition-monitor memory for each type of film deposited. Because this ratio may not accurately be known, the Z-match feature pro-

vided in such monitors may not necessarily be accurate up to high loads. Monitors using the Z-match technique must also keep track of which films have been preloaded before a particular deposition and the impedance of these preloaded samples.

For QCMs submerged in liquids, it has been found that the shear wave loses energy exponentially as it enters the liquid solution. The energy loss adds a term to the Sauerbrey equation, so that frequency shifts Δf do not depend solely on the mass added:

$$\Delta f = -f_0^{3/2} \sqrt{\frac{\eta_s \rho_s}{\pi \mu_Q \rho_Q}}$$

where θ_s and ρ_s are the viscosity and density of the liquid solution, respectively, μ_Q is the shear modulus of quartz (2.947×10^{11} g/cm-s²), and ρ_Q is the density of quartz (2.648 g/cm³). A second crystal in contact with the fluid may compensate for frequency shifts due to viscosity and density of the solution.

As described above, the thickness of a deposited film can be measured as a change in the resonant frequency of a quartz crystal. Figure 12 shows a block diagram of a common method to extract this frequency change. The quartz crystal forms part of a positive feedback oscillator circuit. The output of this circuit is mixed with a reference oscillator not subjected to the film deposition and thus having a constant resonant frequency. The mixer creates a signal in the audio frequency range, which may be counted, or may be input into a frequency-to-voltage converter. The f -to- V converter has the advantage that the output signal can be directly fed into a recorder or computer. Commercial QCM systems are available for less than \$10,000. Many detect mass increments less than 1 ng.

As an alternative to placing the QCM in an oscillator circuit, the QCM may be excited with a signal generator. When the generator is shut off, the crystal exhibits a decaying oscillating behavior characteristic of a high-Q mechanical oscillator. The resonant frequency can be determined from the oscillations within the decaying envelope.

The need for measuring z-values for better Z-matching has introduced more techniques in instrumentation. One technique involves placing the quartz/film resonator to be studied in a circuit where multiple resonances of the device are measured by using a vector voltmeter. (This is a specialized instrument that measures both the amplitude and phase of an oscillating electrical signal.)

Surface Acoustic-Wave Devices

At first glance, a SAW device appears related to the QCM [Fig. 13(a)]. Electrodes are deposited on a piezoelectric quartz wafer, and the crystal is set in oscillation electrically. However, the SAW device is excited only on one surface [Fig. 13(b)], and thus the excited waves occur at the surface, unlike the shear waves propagating in the bulk of a QCM.

However, just as in a QCM, changes in frequency of oscillation occur if mass is deposited on the surface. The frequency shift created by a mass Δm deposited on a SAW crystal of area A is found from

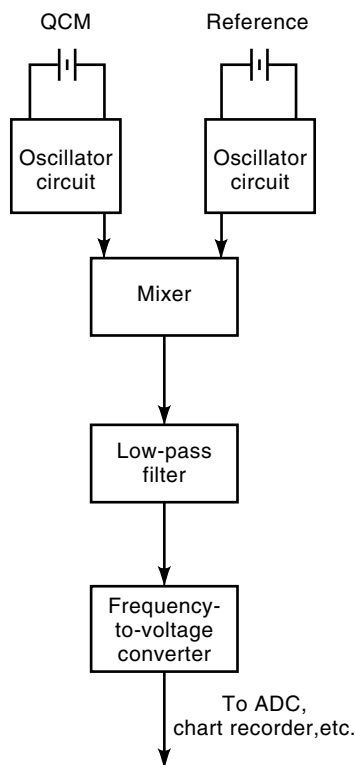


Figure 12. Typical block diagram showing the configuration of a QCM in a film-deposition monitor.

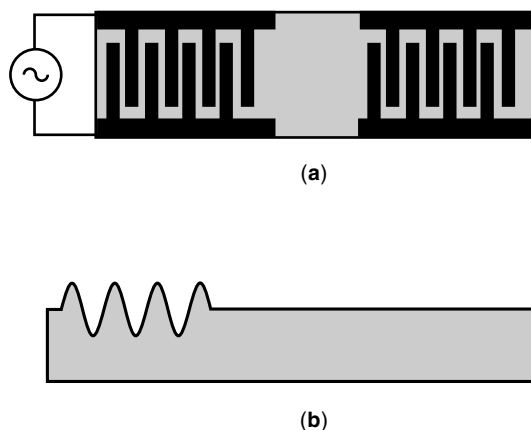


Figure 13. Operation of a surface wave acoustic (SAW) device. (a) Two sets of interdigital transducers are deposited on a quartz substrate. The configuration shown corresponds to an RF delay line. (b) Surface acoustic wave energized by the oscillating voltage source shown in (a).

$$\Delta f = -1.26 \times 10^6 \frac{\text{cm}^2}{\text{Hz} \cdot \text{g}} f_0^2 \frac{\Delta m}{A}$$

where f_0 is the unloaded resonant frequency. The SAW device has two advantages over the QCM. First of all, the SAW is uniformly sensitive to deposits over its entire surface. Secondly, there is no practical limit to the f_0 of the surface waves because the resonant frequency is not determined by crystal thickness. In an SAW device, f_0 is determined by the spacing in the interdigital transducer (IDT) electrodes, which must be smaller and closer together to produce a higher frequency. Thus, the SAW has greater inherent sensitivity than the QCM.

SAWs were initially constructed to serve as delay lines in radio-frequency (RF) circuits, which can be seen in the SAW configuration in [Fig. 13(a)]. One set of electrodes is excited with an RF generator, and the other set receives the signal a short time later. Because the wave speed of surface acoustic waves is far less than the speed of light waves, a short SAW device creates a lengthy delay in the RF signal without appreciable energy loss. SAW devices were soon found impractical for RF applications, however, because they are extremely sensitive to ambient conditions and hence display varying frequency.

SAW devices are incorporated into film-deposition microbalances similarly to QCMs. Typically two separate SAW devices are placed on the same quartz substrate and are excited by a matched pair of RF driver circuits. One of the SAW devices is exposed to the process under study, and the other is a reference. Both signal and reference are mixed, so that the frequency difference is measured in the kilohertz range.

BIBLIOGRAPHY

Balance Types

- W. Sprinkl, E. Lavemann, and H. Ries, An easy-to-build balance for automatic measurement, *J. Phys. E: Sci. Instrum.*, **20**: 1452–1454, 1987.
- G. L. Miller et al., A rocking beam electrostatic balance for the measurement of small forces, *Rev. Sci. Instrum.*, **62**: 705–709, 1992.

- R. M. Schoonover, *Mass Comparator for In-situ Calibration of Large Mass Standards*, *J. Res. Nat. Bur. Stands.*, **90**: 289–294, 1985.
- J. T. Buontempo and F. A. Novak, An inexpensive Wilhelmy balance for the study of Langmuir monolayers, *Rev. Sci. Instrum.*, **63**: 5707–5713, 1992.
- G. T. Gillies and R. C. Ritter, Torsion balances and torsion pendulums, *Rev. Sci. Instrum.*, **64**: 283–309, 1993.
- S. Gordon and C. Campbell, Automatic and Recording Balances, *Anal. Chem.*, **32**: 271R–289R, 1960.

Non-Quartz Crystal Microbalances

- L. Bruschi et al., Novel needle microbalance for adsorption studies, *Rev. Sci. Instrum.*, **68**: 4536–4541, 1997.
- S. J. Suh and H. J. Eun, Small-mass measurement by optical glass-fibre elastic cantilever, *Meas. Sci. Technol.*, **1**: 556–560, 1990.
- L. Bruschi and G. Torzo, A vibrating fibre microbalance for measuring layer-by-layer adsorption on graphite, *Rev. Sci. Instrum.*, **62**: 2772–2777, 1991.
- N. Uetake, T. Asano, and K. Suzuki, Measurement of vaporized atom flux and velocity in a vacuum using a microbalance, *Rev. Sci. Instrum.*, **62**: 1942–1946, 1991.
- D. M. Astill, P. L. Hall, and J. D. C. McConnell, An automated vacuum microbalance for measurement of adsorption isotherms, *J. Phys. E: Sci. Instrum.*, **20**: 19–21, 1987.
- J. E. Sader et al., Method for the calibration of atomic force microscope cantilevers, *Rev. Sci. Instrum.*, **66**: 3789–3798, 1995.
- A. Torii et al., A method for determining the spring constant of cantilevers for atomic force microscopy, *Meas. Sci. Technol.*, **7**: 179–184, 1996.
- L. I. Maissel and R. Glang (eds.), *Handbook of Thin Film Technology*, New York: McGraw-Hill, 1970, pp. 1–103 ff.

Quartz Crystal Microbalances

- D. S. Ballantine and H. Wohltjen, Surface acoustic wave devices for chemical analysis, *Anal. Chem.*, **61**: 704A–712A, 1989.
- M. R. Deakin and D. A. Buttry, Electrochemical applications of QCM, *Anal. Chem.*, **61**: 1147A–1154A, 1989.
- A. Wajid, Improving the accuracy of a quartz crystal microbalance with automatic determination of acoustic impedance ratio, *Rev. Sci. Instrum.*, **62**: 2026–2033, 1991.
- E. Benes, Improved quartz crystal microbalance technique, *J. Appl. Phys.*, **56**: 608–626, 1984.
- P. J. Cumpson and M. P. Seah, The quartz crystal microbalance; radial/polar dependence of mass sensitivity both on and off the electrodes, *Meas. Sci. Technol.*, **1**: 544–555, 1990.
- M. D. Ward and E. J. Delawski, Radial mass sensitivity of the QCM in liquid media, *Anal. Chem.*, **63**: 886–890, 1991.
- Product Review: Quartz crystal microbalances, *Anal. Chem.*, **68**: 625A–628A, 1996.
- M. Rodahl and B. Kasemo, A simple setup to simultaneously measure the resonant frequency and absolute dissipation factor of a quartz crystal microbalance, *Rev. Sci. Instrum.*, **67**: 3238–3239, 1996.
- S. Bruckenstein et al., Dual quartz crystal oscillator circuit. Minimizing effects due to liquid viscosity, density, and temperature, *Anal. Chem.*, **66**: 1847–1852, 1994.
- W. D. Bowers, R. L. Chuan, and T. M. Duong, A 200 MHz surface acoustic wave resonator mass microbalance, *Rev. Sci. Instrum.*, **62**: 1624–1629, 1991.
- W. D. Bowers and R. L. Chuan, Surface acoustic-wave piezoelectric crystal aerosol mass microbalance, *Rev. Sci. Instrum.*, **60**: 1297–1302, 1989.

L. I. WINKLER
Appalachian State University

BALLASTS. See HIGH-FREQUENCY LIGHTING SUPPLIES.

BALLASTS FOR LAMPS. See LIGHTING CONTROL.

BALUNS. See ANTENNA ACCESSORIES.

BAND-GAP NARROWING. See NARROW BAND GAP SEMI-
CONDUCTORS.